神戸大学都市安全研究センター
研究報告，第23号，平成31年３月

Revisiting Inter-seismic Coupling in Southern Japan using Spatially Variable Slip Smoothing Constraints

Francisco Ortega-Culaciati [1),2)]
Shoichi Yoshioka [3)]
Takahiro Akiyama [4)]

Abstract: Geodetic observations, particularly those from space geodesy, can provide continuous and/or dense observations of the different stages of the seismic cycle. Along with a robust slip inversion scheme, such observations provide the means to improve our knowledge of the mechanical behavior and properties of faults. Here we analyze inter-seismic strain accumulation at the subduction zone formed by the subduction of the Philippine Sea plate under the Amurian plate in southern Japan, in order to better understand the distribution of apparent inter-seismic coupling at the subduction interface and its relation with the occurrence of large earthquakes and events associated with aseismic behavior at the megathrust fault. We use inferences of crustal rates at onland GNSS sites from Japan GEONET network to constrain slip deficit rates at the subduction megathrust, using a least squares method in which a spatially variable smoothing constraint was used to obtain robust slip deficit estimates.

Key words: Inter-seismic coupling, GPS, Subduction Zone, Nankai Trough, Japan.

1. INTRODUCTION

The subduction zone in southern Japan is formed by the convergence of the northern margin Philippines Sea plate that is being subducted by the southeastern margin of the continental Amurian plate at the Nankai Trough (see Figure 1). This subduction zone is characterized by a complex geometry of the plate interface, and by a complex partition of surface deformation across several recognized shallow crustal faults. Moreover, megathrust interface has experienced large megathrust earthquakes (Mw > 8) rupturing the shallower portions of the interface, as well as events in which aseismic behavior of the plate interface plays an important role, including slow slip events (SSE's), low frequency tremors, and very low frequency earthquakes. Thus, resembling a very heterogenous mechanical behavior of the subduction interface throughout the entire seismic cycle in the region.

Geodetic observations, particularly those from space geodesy, can provide continuous and/or dense observations of the different stages of the seismic cycle. A careful methodic process of analysis and modeling of such observations is key to achieve a better understanding of the interplay between different geophysical processes occurring during the seismic cycle. In particular, to characterize the mechanical behavior of slip on faults, and to better understand de interaction and causal spatial and temporal relationship between aseismic/seismic slip behavior at the different portions of a fault, as well as the interaction of such fault related processes with its surrounding media and other faults.

Here we are concerned on a achieving a better understanding of the physical processes, occurring in the portion of the subduction megathrust formed by the subduction of the Philippine Sea plate under the Amurian plate in southern Japan, that are responsible for controlling strain accumulation that eventually is released in episodes associated to earthquake occurrence or dominated by aseismic behavior of the subduction interface. Particularly, we analyze estimates of apparent coupling at the subduction interface, constrained by onland GNSS inferred crustal rates, with the ultimate goal of improving our knowledge on its spatial distribution of frictional properties at the subduction megathrust.

In the following, we present preliminary results of our model representing inter-seismic strain accumulation at the Nankai Trough subduction margin, in terms of slip deficit rates estimated for the subduction interface in a region delimited by the Bungo channel located westwards of Shikoku island, and the eastern flank of the Kii Peninsula, where convergence rate has been reported to vary from 5 to 6 [cm/yr] (Loveles and Meade, 2010 and references therein). We compare our results with reports of seismic and aseismic behavior at the subduction megathrust, and make interpretations in terms of the frictional rheology of the plate interface.

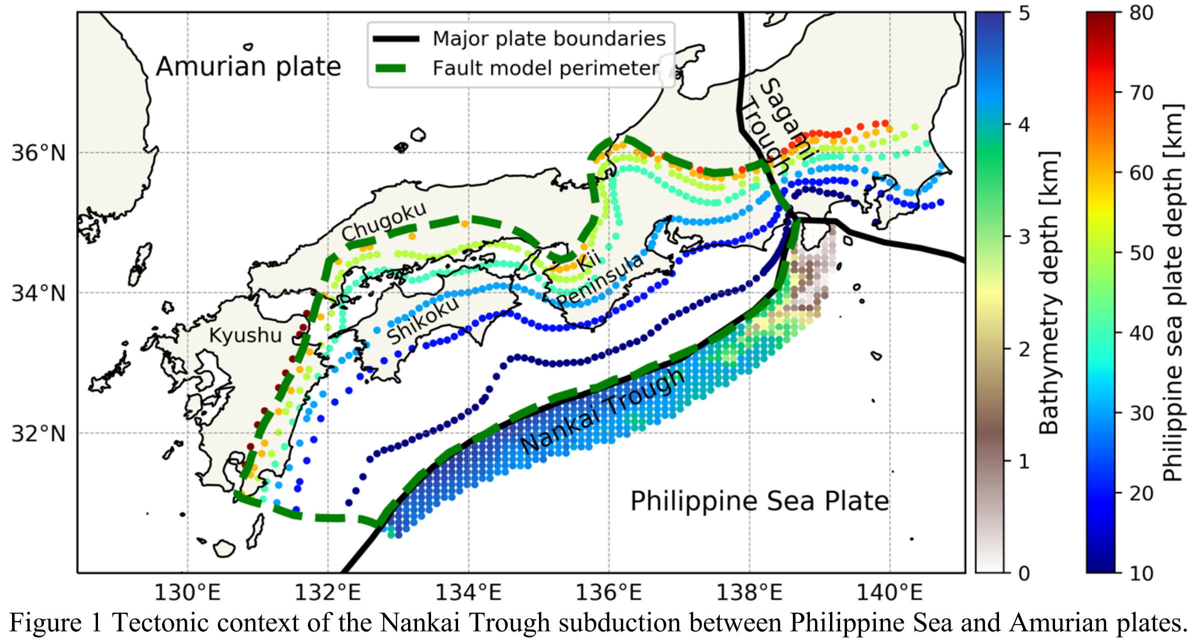

Figure 1 Tectonic context of the Nankai Trough subduction between Philippine Sea and Amurian plates. Colored contours indicate depth of top boundary of Philippine Sea Plate (see text 1 and 2.2 for further details). Bathymetry is shown near the Nankai Trough is used to partially constrain the 3D geometry of the Philippine sea plate.

2. DATA AND METHODS

2.1 GNSS observations of crustal deformation

We use GNSS data obtained from the Information Authority of Japan (GSI), in the form of F3 daily solutions (Nakagawa et al., 2009), from January 2002 to December 2010, at 581 GNSS stations in southern Japan. For each GNSS station, there are three time series available, one for each of the three components (East, North, Up). Each time series contain signals coming from different physical sources at diverse spatial and temporal scales. Among such sources, we are interested in the ones related to geophysical processes, anthropogenic and errors coming from the design of the GNSS positioning system. For daily positional time series, geophysical signals may include tectonic plate motion, earthquake associated deformation (co- and post-seismic deformation), slow transient motion associated to the occurrence of events of aseismic dislocation in faults (e.g., slow slip events), secular motion caused by inter-seismic tectonic loading, quasi-periodic signals associated with hydrological forcing (a.k.a., seasonal motion), transient signals related to volcanic processes, etc. Also, changes in hardware of the GNSS receivers might cause apparent discontinuities in the positional signal. Moreover, human activity such as agriculture, construction or mining (among others) can modify the surroundings of a GNSS receiver, producing ground deformation or changes in the scattering patterns of the signals received from the GNSS satellites, and hence producing a signal in the positional time series, that can be a true or apparent motion, respectively. In the other hand, there are also apparent motions that are coherent across the whole considered GNSS network. Such motions are referred to as Common Mode Error (CME). CME may be interpreted as errors in the determination of the reference frame for each epoch of the time series, produced by uncertainties in the position of the GNSS satellites as well as in satellite clocks. CME ranges from a few millimeters to centimeters, thus its identification and removal is essential if our eventual goal is to identify subtle tectonic signals.

Extending the approach of Yoshioka et al. (2004), we separate secular rates due tectonic loading in southern Japan by modeling GNSS positional time series using the following equation,

$$y(t) = a_0 + \sum_{i}^{n} a_i\, T_i(t) + b \sin\left(\frac{2\pi t}{T}\right) + c \cos\left(\frac{2\pi t}{T}\right) + d \sin\left(\frac{4\pi t}{T}\right) + e \cos\left(\frac{4\pi t}{T}\right) + H(t) \quad (1)$$

where $T_i(t)$ is Chebyshev polynomials, and constants a_0, a_i , b, c, d, and e are determined using least squares methodology to adjust model (1) to the GNSS positional time series. Optimal value of n is determined using AIC (Akaike, 1973). Trigonometric functions model annual and semi-annual seasonal signals (T = 1 year) and H(t) is a linear combination of Heaviside functions representing the discontinuities found in the time series. In an iterative manner, we estimated CME from the time series resulting as a residual between observed positional time series and predicted ones using adjusted model (1). On each iteration, the model is fitted and CME re-estimated and removed from observed time series to be used to fit the model in the next iteration in which new features might be added to H(t). From the fit process, we obtain estimates of crustal velocities, resembling secular rates and possible slow motions, that are referred to GNSS station 950382 by subtracting velocities estimated at such GNSS site from the estimated at all other GNSS stations. Figure 1 show our estimates of secular rates referenced at GNSS site 950382. For this preliminary study, we chose to calculate secular rates as the displacements of the GNSS stations that occurred during the year 2009. Note that although the estimated rates might contain slow motions, those are not observed during the year 2009, thus allowing us to use inferred crustal velocities to estimate slip deficit rates representative for such year.

2.2 Crustal deformation model

We build a 3D subduction elastic system by the use of the backslip model (Savage, 1983). We use depth contour information of the top of the Philippine sea plate and its bathymetry near the Nankai Trough (see Figure 1) to construct a 3D model of the Amurian-Philippine plates interface at southern Japan. The depth contours for southwestern Japan were computed by Baba et al. (2002), Hirose et al. (2008), Nakajima and Hasegawa (2007), for Kanto district by Hirose et al. (2008a), and for the northern area of the Izu island by Nakajima et al. (2009) and retrieved from Fuyuki Hirose web page (http://www.mri-jma.go.jp/Dep/st/member/fhirose/en/en.PHS.html). We fit the aforementioned depth data by a geometric model conformed by 2D B-splines basis functions. Then, we perform a triangulation of the 3D geometric

(a)

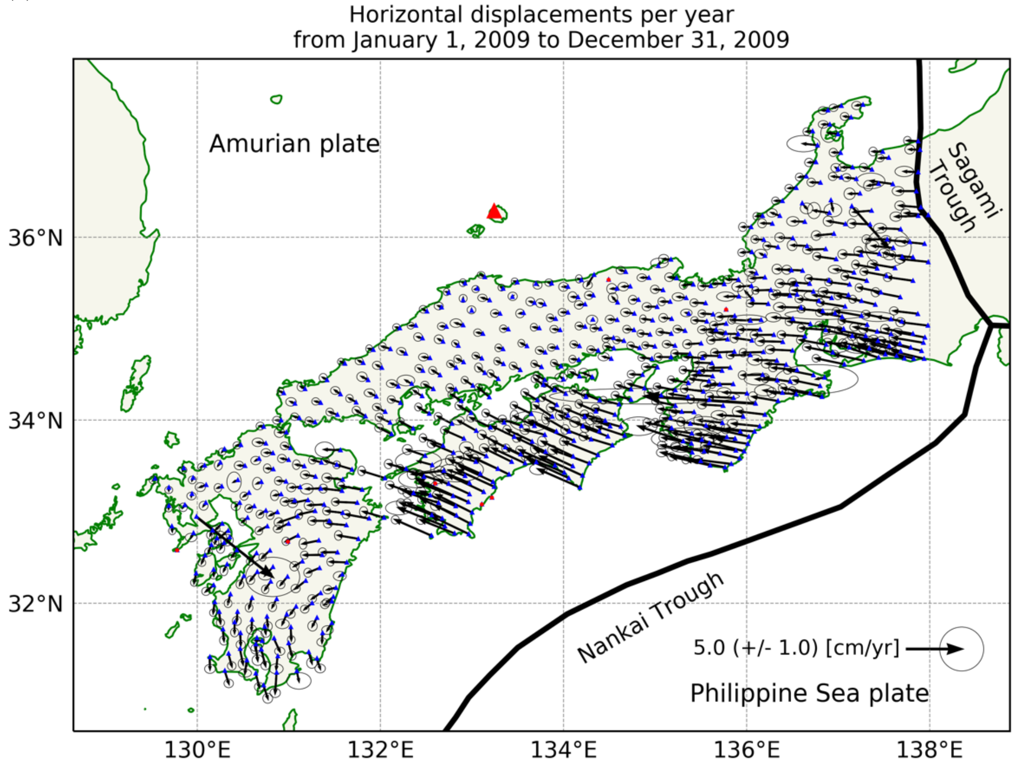

(b)

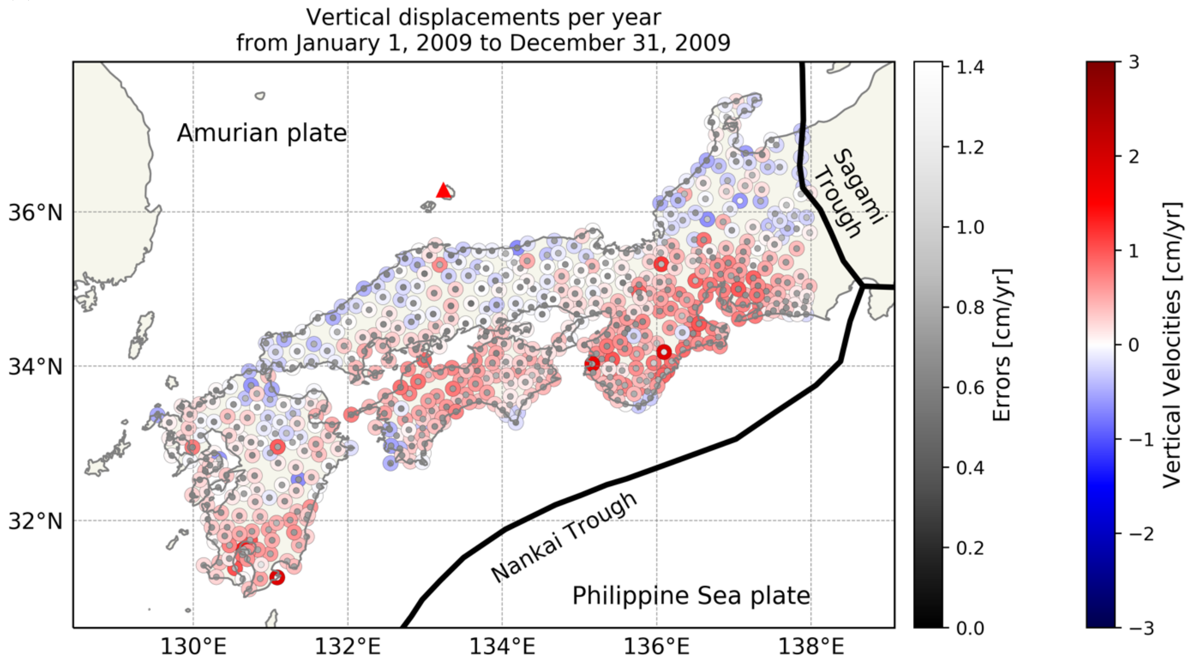

Figure 2. Horizontal (a) and vertical (b) crustal velocities used in this study as obtained from GNSS observations from GEONET network (Sagiya et al., 2000) in southern Japan for the year 2009. Horizontal velocities are shown with error ellipses of one standard deviation. Vertical velocities are show in concurrent colored circles, the external circle showing velocity value (positive upwards) and interior circle indicates measurement error in gray colors. Red triangle indicates GNSS station to which crustal velocities referred.

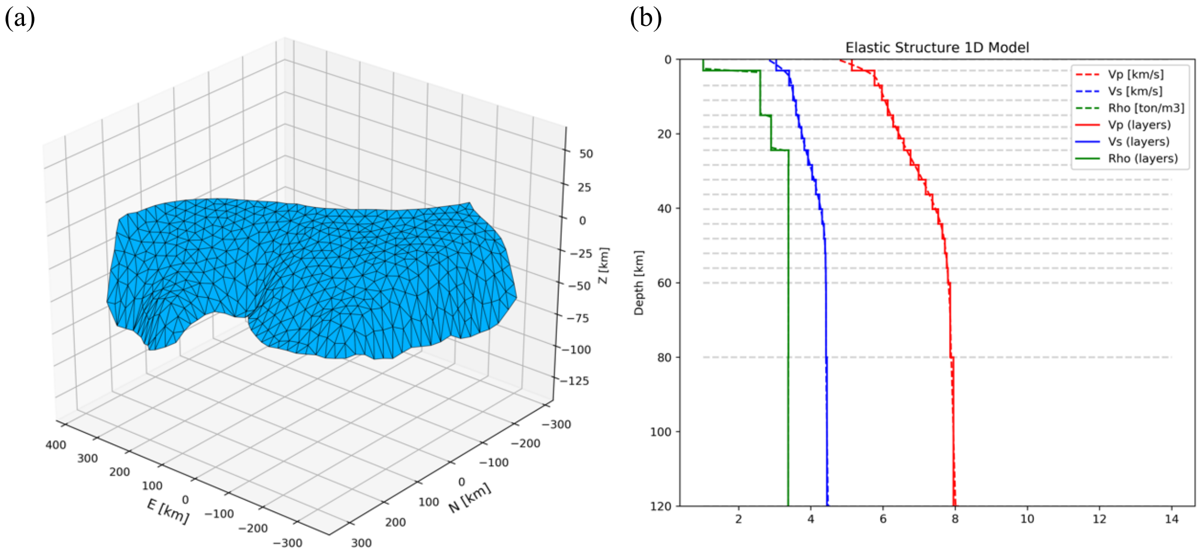

Figure 3 (a) 3D view of a triangulated surface used to represent fault slip. (b) Elastic structure used to model slip in an elastic layered media. In (b), Dashed lines show Vp (red) and Vs (blue) body wave propagation velocity from JMA2001 velocity structure model (Ueno et al. 2002) and density of the media from the Preliminary Reference Earth Model – PREM (Dziewonski and Anderson 1981). Solid lines show piecewise constant values for elastic parameters averaged at each layer of the media with boundaries shown as horizontal dashed gray lines.

model within the fault border shown in Figure 1, using a 3D triangulation fault mesh generator for fault slip modeling (Ortega-Culaciati, in preparation), to produce the 3D triangulated fault mesh shown in Figure 3a, in which each triangular element has a characteristic size of about 20 km.

Slip is assumed to be uniformly distributed within each triangular fault element. Also, slip is parameterized at two orthogonal directions at each fault patch: a slip component that has a rake of the slip vector whose horizontal (map) projection is parallel to the average direction of convergence between Philippine and Amurian plates in the study area (azimuth = -58º), and a component in an orthogonal direction within the fault element. We name these fault slip directions as rake parallel and rake perpendicular directions.

Strain accumulation due to inter-seismic tectonic loading at the Amurian – Philippine plate interface is represented using the backslip model (Savage, 1983). Green functions, corresponding to the rate of crustal displacement for each direction of each GNSS station due to unit slip deficit rate on each triangular fault element slip direction, are computed using a stratified isotropic elastic media (see Figure 3b) using Computer Programs in Seismology (Herrmann, 2013).

As the inferred crustal velocities are referred to GNSS site 950382 in the Amurian plate, a reference frame correction is modeled for the crustal velocities in order to produce a translation and rotation to a reference frame consistent with the convergence motion between Philippine Sea Plate and the portion of the Amurian plate where southern Japan is located. The reference frame correction is performed using a ridig motion of a spherical plate (e.g., Cox and Hart, 1986), in which cartesian coordinates of the Euler pole describing the motion are used as parameters to define the rigid motion. While we recognize that internal deformation, surface fault behavior and block motion is complex in southern Japan (e.g., Wallace et al., 2009; Loveless and Meade, 2010; Nishimura, 2011), as in this preliminary study we are interested in studying inter-seismic coupling at the Nankai Trough subduction in front of Shikoku island and Kii Peninsula, the aforementioned rigid motion will be also used as a rough, but sufficient, approach to correct for block motion and analyze inter-seismic coupling in such areas.

2.3 Inversion Methodology

We estimate slip deficit rates at the subduction interface between Amurian and Philippine Sea plates as well as the cartesian coordinates of the Euler pole describing the reference frame correction and average rigid block motion in the region, both constrained by crustal rates measured at the GNSS sites shown in Figure 2. The slip estimation process is carried out by solving the linear least squares problem,

$$\min_{\boldsymbol{m}} \left\|\mathbf{W}_{\chi}(\mathbf{Gm}-\mathbf{d})\right\|_2^2 + \varepsilon^2\|\mathbf{Lm}\|_2^2 \tag{2}$$

composed of 2 terms, the first norm measuring the goodness of the fit between observations $\mathbf{d}$ and model prediction $\mathbf{Gm}$, and the second term corresponding to the regularization needed in order to solve the inherently ill-posed slip inversion problem (e.g., Hansen, 1998). Here ε^2 is a regularization or damping parameter that controls trade-off between physical ($\mathbf{Gm}=\mathbf{d}$) and regularization ($\mathbf{Lm}=\mathbf{0}$) equations, determined using the L-curve model selection method (Hansen, 1993). The vector of model parameters is

$$\mathbf{m} = \begin{bmatrix}\mathbf{m}_{\mathbf{BSpar}}^{\mathsf{T}} & \mathbf{m}_{\mathbf{BSperp}}^{\mathsf{T}} & \mathbf{m}_{\mathbf{E}}^{\mathsf{T}}\end{bmatrix}^{\mathsf{T}} \tag{3}$$

where $\mathbf{m}_{\mathbf{BSpar}}$ corresponds to the rake parallel backslip, $\mathbf{m}_{\mathbf{BSperp}}$ to the rake perpendicular backslip at each triangular fault element, and $\mathbf{m}_{\mathbf{E}}$ to the model parameters associated to the cartesian components of the Euler pole modeling crustal rate corrections.

For the first term in (2), $\mathbf{G}$ is the Green's functions matrix, $\mathbf{m}$ a vector of model parameters to be estimated, $\mathbf{d}$ a vector containing the GNSS observations of crustal rates, $\mathbf{W}_{\chi}$ a data weight matrix such that $\mathbf{W}_{\chi}^{\mathsf{T}}\mathbf{W}_{\chi} = \mathbf{C}_{\chi}^{-\mathbf{1}}$, where $\mathbf{C}_{\chi} = \mathbf{C}_{\mathbf{d}} + \mathbf{C}_{\mathbf{p}}$ is the data misfit covariance matrix in which errors on observations $\mathbf{C}_{\mathbf{d}}$ and physical backslip model prediction $\mathbf{C}_{\mathbf{p}}$ are considered. For $\mathbf{C}_{\mathbf{d}}$ we consider a diagonal matrix with variances obtained during the estimation of the crustal rates. Model prediction errors are shown to be proportional to backslip model prediction (Minson et al., 2013; Duputel et al. 2014), but for practicality purposes on the slip inversion process, as for the solution of the inversion problem we expect to explain well the observations, backslip model prediction errors are taken proportional (10%) to the crustal rate observations (Minson et al., 2013), so we use $\mathbf{C}_{\mathbf{p}} = 0.1\ \mathrm{diag}(\mathbf{d})$. Here, the Green's functions matrix is

$$\mathbf{G} = [\mathbf{G}_{\mathbf{BSpar}} \quad \mathbf{G}_{\mathbf{BSperp}} \quad \mathbf{G}_{\mathbf{E}}] \tag{4}$$

where $\mathbf{G}_{\mathbf{BSpar}}$ is the Green's functions matrix for rake parallel backslip, $\mathbf{G}_{\mathbf{BSperp}}$ for rake perpendicular backslip and $\mathbf{G}_{\mathbf{E}}$ for the cartesian components of the Euler pole describing crustal rate corrections.

For the regularization term in (2), $\mathbf{L}$ includes a soothing constraint on backslip, without imposing any constraint on the cartesian components of the Euler vector modeling the crustal rates corrections. In terms of model parameter vector, the regularization operator can be written as

$$\mathbf{L} = \begin{bmatrix}\mathbf{S}^{-\frac{1}{2}}\boldsymbol{\nabla}^2 & \mathbf{0} & \mathbf{0} \\ \mathbf{0} & \sigma^{-2}\mathbf{I} & \mathbf{0}\end{bmatrix} \tag{5}$$

where $\boldsymbol{\nabla}^{\mathbf{2}}$ is a finite difference approximation of the Laplacian differential operator, and $\mathbf{S} = \frac{\mathrm{diag}(\boldsymbol{P})}{\mathbf{max}(\mathbf{diag}(\mathbf{P}))}$ is the Sensitivity matrix and $\mathbf{P} = \mathbf{G}_{\mathbf{BSpar}}^{\mathsf{T}}\ \mathbf{C}_{\chi}\ \mathbf{G}_{\mathbf{BSpar}}$ is the precision matrix of the unregularized inversion problem for the rake parallel component of slip. The Sensitivity matrix weights the Laplacian of the rake parallel component of backslip in order to provide a spatially variable smoothing constraint that is stronger at the fault portions least constrained by the observations (Ortega-Culaciati, 2013). The spatially variable smoothing allows for a better recovery of backslip at the portions of the fault well constrained by observations (closer to coastline when only onland measurements are available), while stabilizing slip estimates at the least constrained regions of the fault, corresponging to near trench portions when only onland data is used to constrain slip at the megathrust fault (Ortega-Culaciati, 2013). In the other hand, the term $\sigma^{-2}\mathbf{I}$ in (5) is the regularization term for rake perpendicular component of backslip. Here we ask for small values (close to 0) of rake perpendicular backslip with an a priori error that we set equal to $\sigma = 0.2$ [cm/yr], thus allowing only small values of slip in such direction for backslip estimates, as we expect backslip to occur mainly along plate convergence direction. Following Tarantola (2005), the solution of problem (2) is obtained as,

$$\mathbf{m} = \left(\mathbf{G}^{\mathsf{T}}\mathbf{C}_{\chi}\mathbf{G} + \varepsilon^2\mathbf{L}^{\mathsf{T}}\mathbf{S}^{-1}\mathbf{L}\right)^{-1}\mathbf{G}^{\mathsf{T}}\mathbf{C}_{\chi}\mathbf{d} \tag{6}$$

with a posteriori covariance matrix of estimated model parameters,

$$\mathbf{C}_{\mathbf{m}} = \left(\mathbf{G}^{\mathsf{T}}\mathbf{C}_{\chi}\mathbf{G} + \varepsilon^2\mathbf{L}^{\mathsf{T}}\mathbf{S}^{-1}\mathbf{L}\right)^{-1} \tag{7}$$

3. RESULTS AND DISCUSSION

Figure 4a show obtained estimates of backslip (or slip deficit) rates at the plate boundary between Amurian and Philippine Sea plates. Figures 4a and 4b show GNSS inferred crustal rates (horizontal component fixed by the reference frame correction estimated during inversion) compared with the crustal rate prediction of the backslip model obtained during the inversion process, for horizontal and vertical components respectively.

We observe that horizontal crustal velocities are well explained by the model predictions in the region of the Nankai Trough subduction between the Bungo Channel (~132ºE) and the eastern limit of the Kii Peninsula (~137ºE). Nevertheless, horizontal data is poorly explained at the GNSS sites on Kyushu and for the ones located near the eastern limit of the Nankai Trough, possibly due to effects of large block rotation (e.g., Loveless and Meade, 2010) and the influence of tectonic loading due to the Japan Trench megathrust subduction and deformation processes occurring from the Sagami Trough to the East, both which are not currently accounted in our modeling. In the other hand, vertical data is poorly explained, with the exception of some GNSS sites near the southern coast of Shikoku and Kii Peninsula, possibly due to larger errors on vertical observation caused by a high variability of the daily positions of vertical positions compared to horizontal ones in the GNSS time series.

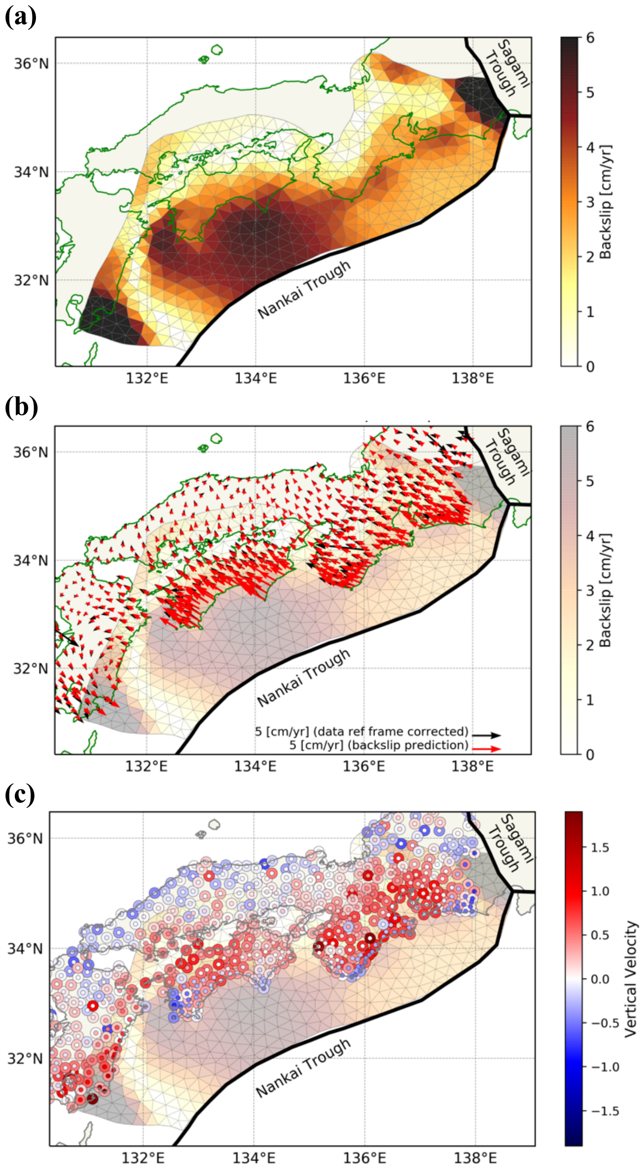

Figure 4 Estimates of backslip (a) constrained by GNSS inferred crustal velocities shown in Figure 1, resembling inter-seismic slip deficit at the Philippine sea plate subduction interface. Note that the color bar saturates at average plate convergence value of 6 [cm/yr]. Panel (b) shows the backslip model crustal horizontal component of the velocity prediction compared against observed values, shown as red and black arrows respectively. Horizontal observations are corrected by the reference frame correction estimated during backslip inversion. Panel (c) compares backslip model prediction and observations of vertical crustal velocities as colored concurrent circles. Outer circle corresponds to observations and inner circles to model predictions. Positive velocities indicate uplifting of the crust. Nankai and Sagami troughs are shown as black lines.

The backslip model estimated in this work, between the Bungo channel (~132ºE) and the eastern limit of the Kii Peninsula (~137ºE), show slip deficit rates with peak amplitudes of about ~ 6 [cm/yr] and backslip direction that are both similar to the relative motion between the Philippine Sea plate and the portion of the Amurian plate where the studied region of Japan is located (see Loveless and Meade, 2010 and references therein). Nevertheless, at the north-eastern and south-western limits of the modeled fault surface, backslip estimates are much higher, reaching peak values of about 8.5 and 12 [cm/yr], respectively. At the north-eastern flank, high backslip is trying to explain unmodeled effects caused by tectonic loading due to the Japan Trench megathrust subduction and deformation processes whose signature on the analyzed GNSS network sites has origin on a region located from the Sagami Trough to the East. At the south-western flank, besides the high unrealistic value of 12 [cm/yr], slip is oriented contrary to the expected direction of plate convergence, and occurs because the slip model tries to explain data affected by a large rotation rate of the crustal block that includes the southernmost part of Kyushu (e.g., Loveless and Meade, 2010; Nishimura et al., 2018). Our backslip estimates at the aforementioned regions are thus biased and unreliable due to unmodeled crustal motions near those regions. Figure 5 shows our estimates of backlip where unreliable artifacts of the inversion are shown as hatched gray areas. Also, in Figure 5 we compare our backslip estimates along with historical large earthquakes, slow slip events and very low frequency events occurred in the study area.

Regarding the errors of the presented backlip model, one advantage of using the spatially variable smoothing constraint is that errors on model estimates tend to show little variations through the whole fault surface, which is achieved by a fault variable spatial correlation length of backslip estimates as a result of empirically modulating the strength of the smoothing constraint by the Sensitivity of fault slip (Ortega-Culaciati, 2013). Here errors on backslip estimates range from 0.8 [cm/yr] for the fault elements near the coast line, to 1.1 [cm/yr] for the ones near the trench. Also, backslip estimates are averaging the "true" or unknown backslip model (what physically happened at the subduction interface and we are attempting to infer) over a region with a characteristic radii size indicated by a correlation length of about 8 [km] near the coast and about 60 [km] near the trench.

Several inter-plate coupling models have been proposed for the region (e.g., Loveless and Meade, 2010; Yoshioka and Matsuoka, 2013; Yokota et al., 2016; Nishimura et al., 2018). Among those models, our slip deficit rates are more similar to the model estimated by Yokota et al. (2016). In contrary to our modeling that only uses onland GNSS observations from GEONET network to constrain backslip estimates, Yokota et al. (2016) uses also seafloor secular rates obtained from a seafloor observation network developed using a combined global positioning system and acousting ranging (GPS-A) technique (see Yokota et al., 2016 and references therein). The similarities of both models show the usefulness of the spatially variable, sensitivity based, regularization technique applied in this work to better constrain slip at the fault portions located further away from onland GNSS observations.

Our model shows a region of high slip deficit between near the coast of Shikoku up to near trench, coinciding with the location of the source of the 1946 Mw 8.3 Nankai earthquake estimated by Sagiya and Tatcher (1999). Also, regions of high coupling offshore the Kii Peninsula up to mid distance between shore and the Nankai Trough, coincide with source region of the 1944 Mw 8.1 Tonankai earthquake as estimated by Sagiya and Tatcher (1999). In terms of a "rate and state" friction formalism (e.g., Lay & Kanamori, 1984; Perfettini & Avouac, 2004), those inferred regions of high slip deficit are consistent with a velocity strengthening frictional regime, thus allowing the occurrence of the 1944 and 1946 earthquakes. In the other hand, we find a region of high coupling at the Bungo channel, where several slow slip events have occurred in the past (e.g., Yoshioka et al., 2015). Such a behavior could be still explained under the rate and state formulism, but brittle and ductile behavior segmentation at the megathrust might be obscured by the smoothing constraints typically used in fault slip inversion. Also, such region of high slip deficit might be an artifact due to ignoring block motion at Kyushu. Further future analysis is needed to understand which of beforementioned hypotheses might be dominant but is out of the scope of this work.

In a similar manner, we find that within deeper regions of the plate interface resembling a transition between fully coupled interface (slip deficit near plate convergence) and uncoupled (near null slip deficit) interface located beneath, several long-term slow slip events (LT-SSE's) occur. Also, at the deeper edge of the transition zones, beneath regions of high coupling, several short-term slow slip events occur. Thus, suggesting a very heterogenous distribution of frictional behavior at the subduction interface. A similar interpretation can be given at shallower portions of the megathrust, where in regions of mild or very low coupling show evidence of very low frequency earthquake

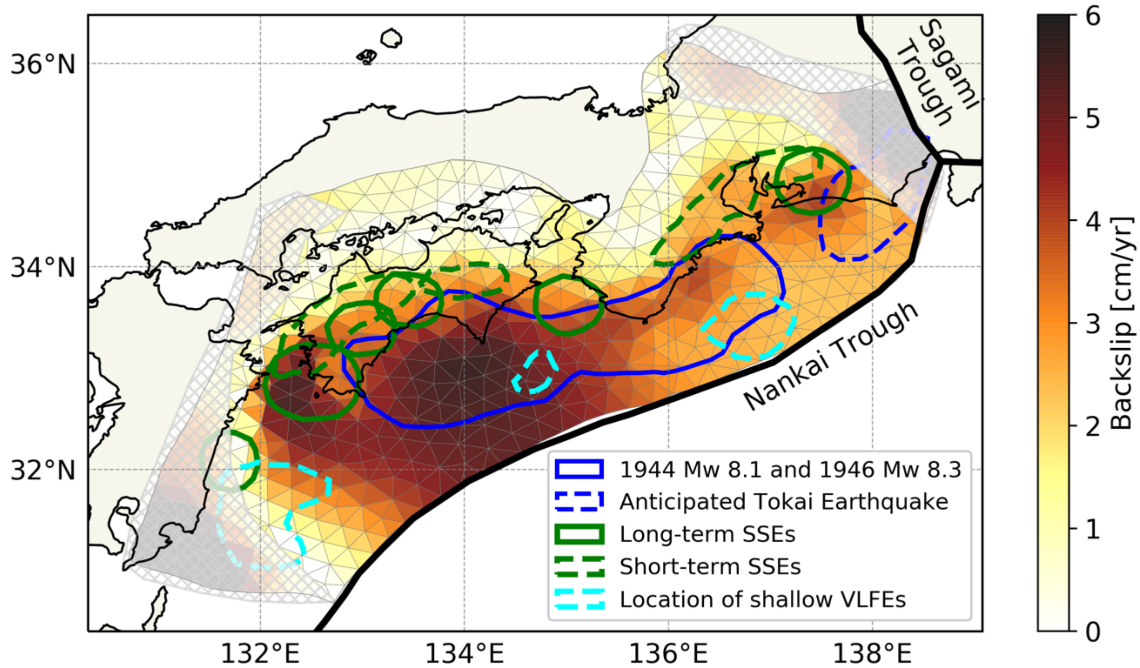

Figure 5 Estimates of backslip constrained by GNSS inferred crustal velocities shown in Figure 1, resembling inter-seismic slip deficit at the Philippine sea plate subduction interface. Shaded areas mask regions in which backlip estimated are considered to be biased and thus unreliable (see main text). Nankai and Sagami troughs appear as thick black lines. Colored lines indicated in the legend and explained below were digitized from Figure 11 in Nishimura et al. (2018). Blue line resembles the rupture region of the 1944 Mw 8.1 Tonankai and 1946 Mw 8.3 Nankai earthquakes (Sagiya and Thatcher, 1999). Dashed blue line represents location of the rupture area for a potential future earthquake suggested by Nishimura et al. (2018). Solid green lines encompass regions that have experienced long term slow slip events (Ozawa et al. 2013; Yarai and Ozawa, 2013; Kobayashi, 2014, Yoshioka et al. 2015; Takagi et al. 2016). Dashed green lines indicate regions of the megathrust with occurrence of short-term slow slip events (Nishimura et al., 2014; Ozawa et al, 2014). Cyan dashed lines show location of shallow very low frequency earthquakes from Nishimura et al. (2018).

4. CONCLUSIONS

We estimated inter-seismic slip deficit rates for the portion of the Nankai Trough subduction between the Bungo Channel and eastern coast of the Kii Peninsula, constrained by onland GNSS derived secular crustal rates for year 2009. Our estimates are consistent with previous knowledge of past earthquakes and aseismic behavior in the region, as well as with a very heterogeneous mechanical behavior at the subduction interface. Although our modeling only includes onland GNSS observations and a rough rigid motion correction for both reference frame and onland block motion, our results are very similar to studies in which not only internal deformation and block motion are considered but also seafloor geodetic measurements of inter-seismic seafloor deformation. We believe that similarities observed between aforementioned models are achieved because the inclusion of a spatially variable regularization, that allows the obtaining of robust slip estimates at the regions located further away from onland geodetic observations (at fault portions near the trench). However, while the used inversion and regularization technique shows great potential to improve interplate coupling estimates, we recognize that our preliminary modeling needs to be improved by including complex behavior of block motion and internal deformation inferred by other authors in southern Japan as well as to include reported geodetic observations describing the motion of the seafloor. Such improvements will result of continued future collaboration between the co-authors of this work.

ACKNOWLEDGEMENTS

Support from the Research Center for Urban Safety and Security, Kobe University, Japan enabled the successful development of the modeling carried out in this work as well as to allow the stablishment of scientific collaboration between the co-authors by providing the means for the Visiting Researcher position of Francisco Ortega-Culaciati at Kobe University. We acknowledge NLHPC as this research calculations were partially done using the supercomputing infrastructure of the NLHPC (ECM-02) at University of Chile.

REFERENCES

Akaike, H. (1973), Information theory and an extension of the maximum likelihood principle, 2nd Inter. Symp. On Information Theory (Petrov, B. N. and Csaki, F. eds.), Akademiai Kiado, Budapest, 267-281.

Baba, T., Y. Tanioka, P. R. Cummins, and K. Uhira (2002), The slip distribution of the 1946 Nankai earthquake estimated from tsunami inversion using a new plate model, Phys. Earth Planet. Inter., 132, 59-73.

Cox, A., and R. B. Hart (1986), *Plate tectonics: how it works*, Palo Alto: Blackwell Scientific Publications.

Duputel, Z., P. S. Agram, M. Simons, S. E. Minson, and J. L. Beck (2014), Accounting for prediction uncertainty when inferring subsurface fault slip, *Geophysical Journal International*, *197*(1), 464–482, doi:10.1093/gji/ggt517.

Dziewonski, A. M., and D. L. Anderson (1981), Preliminary reference Earth model, *Physics of the Earth and Planetary Interiors*, *25*(4), 297–356, doi:10.1016/0031-9201(81)90046-7.

Hansen, P. C., & O'Leary, D. P. (1993). The use of the L-curve in the regularization of discrete ill-posed problems. SIAM Journal on Scientific Computing, 14(6), 1487– 1503.

Hansen, P. C. (1998). Rank-Deficient and Discrete Ill-Posed Problems: Numerical Aspects of Linear Inversion. SIAM, Philadelphia.

Herrmann, R. B. (2013), Computer programs in seismology: An evolving tool for instruction and research, *Seism. Res. Lettr.* **84**, 1081-1088, doi:10.1785/0220110096

Hirose, F., J. Nakajima, and A. Hasegawa (2008), Three-dimensional seismic velocity structure and configuration of the Philippine Sea slab in southwestern Japan estimated by double-difference tomography, J. Geophys. Res., 113, B09315, doi:10.1029/2007JB005274.

Hirose, F., J. Nakajima, and A. Hasegawa (2008a), Three-dimensional velocity structure and configuration of the Philippine Sea slab beneath Kanto district, central Japan, estimated by double-difference tomography, J. Seism. Soc. Jpn., 2, 60, 123-138. (in Japanese with English abstract).

Kobayashi, A. (2014), A long-term slow slip event from 1996 to 1997 in the Kii Channel, Japan, *Earth Planets and Space*, *66*(1), 143–7, doi:10.1186/1880-5981-66-9.

Lay, T., & Kanamori, H. (1981). An asperity model of large earthquake sequences. In *Maurice Ewing Series* (Vol. 4, pp. 579–592). Washington, D. C.: American Geophysical Union. http://doi.org/10.1029/ME004p0579

Loveless, J. P., and B. J. Meade (2010), Geodetic imaging of plate motions, slip rates, and partitioning of deformation in Japan, *Journal of Geophysical Research*, *115*(B2), B02410, doi:10.1029/2008JB006248.

Minson, S. E., M. Simons, and J. L. Beck (2013), Bayesian inversion for finite fault earthquake source models I--theory and algorithm, *Geophysical Journal International*, *194*(3), 1701–1726, doi:10.1093/gji/ggt180.

Nakagawa, H., Toyofuku, T., Kotani, Kyoko, Miyahara, B., Iwashita, C., Kawamoto, S., Hatanaka, Y., Munekane, H., Ishimoto, M., Yutsudo, T., Ishikura, N., Sugawara, Y., 2009. Development and validation of GEONET new analysis strategy (version 4). Bulletin Geographic Survey Institute 118, 1–8 (in Japanese).

Nakajima, J., and A. Hasegawa (2007), Subduction of the Philippine Sea plate beneath southwestern Japan: Slab geometry and its relationship to arc magmatism, J. Geophys. Res., 112, B08306, doi:10.1029/2006JB004770.

Nakajima, J., F. Hirose, and A. Hasegawa (2009), Seismotectonics beneath the Tokyo metropolitan area, Japan: Effect of slab-slab contact and overlap on seismicity, J. Geophys. Res., 114, B08309, doi:10.1029/2008JB006101.

Nishimura, T., 2011, Back-arc spreading of the northern Izu-Ogasawara (Bonin) Islands arc clarified by GPS data: Tectonophysics, v. 512, p. 60–67, https://doi.org/10.1016/j.tecto.2011.09.022.

Nishimura, T., Sato, M., and Sagiya, T., 2014, Global Positioning System (GPS) and GPS-Acoustic observations: Insight into slip along the subduction zones around Japan: Annual Review of Earth and Planetary Sciences, v. 42, p. 653–674, https://doi.org/10.1146/annurev-earth-060313 -054614.

Nishimura, T., Y. Yokota, K. Tadokoro, and T. Ochi (2018), Strain partitioning and interplate coupling along the northern margin of the Philippine Sea plate, estimated from Global Navigation Satellite System and Global Positioning System-Acoustic data, *Geosphere*, *14*(2), 535–551, doi:10.1130/GES01529.1.

Ortega-Culaciati, F. H. (2013). Aseismic Deformation in Subduction Megathrusts: Central Andes and North-East Japan (Ph.D. dissertation). California Institute of Technology, Pasadena, California, USA.

Ozawa, S., H. Yarai, T. Imakiire, and M. Tobita (2013), Spatial and temporal evolution of the long-term slow slip in the Bungo Channel, Japan, *Earth Planets and Space*, *65*(2), 67–73, doi:10.5047/eps.2012.06.009.

Perfettini, H., & Avouac, J. P. (2004). Postseismic relaxation driven by brittle creep: A possible mechanism to reconcile geodetic measurements and the decay rate of aftershocks, application to the Chi-Chi earthquake, Taiwan. *Journal of Geophysical Research: Solid Earth (1978–2012)*, *109*(B2). http://doi.org/10.1029/2003JB002488.

Sagiya, T., S. Miyazaki, and T. Tada (2000), Continuous GPS array and present-day crustal deformation of Japan, *Pure and applied Geophysics*, *157*(11-12), 2303–2322.

Sagiya, T., and W. Thatcher (1999), Coseismic slip resolution along a plate boundary megathrust: The Nankai Trough, southwest Japan, *Journal of Geophysical Research*, *104*(B1), 1111–1129.

Sella, G. F., T. H. Dixon, and A. Mao (2002), REVEL: A model for recent plate velocities from space geodesy, *Journal of Geophysical Research*, *107*(B4), 2081, doi:10.1029/2000JB000033.

Takagi, R., K. Obara, and T. Maeda (2016), Slow slip event within a gap between tremor and locked zones in the Nankai subduction zone, Geophys. Res. Lett., 43, 1066–1074, doi:10.1002/2015GL066987.

Ueno, H., S. Hatakeyama, T. Aketagawa, J. Funasaki, and N. Hamada (2002), Improvement of hypocenter determination procedures in the Japan Meteorological Agency, *Q. J. Seismol.*, *65*, 123–134.

Wallace, L., Ellis, S., Miyao, K., Miura, S., Beavan, J., and Goto, J., 2009, Enigmatic, highly active left-lateral shear zone in southwest Japan explained by aseismic ridge collision: Geology, v. 37, p. 143–146, https://doi.org/10.1130/G25221A.1.

Yarai, H., and S. Ozawa (2013), Quasi-periodic slow slip events in the afterslip area of the 1996 Hyuga-nada earthquakes, Japan, *J Geophys Res-Sol Ea*, *118*(5), 2512–2527, doi:10.1002/jgrb.50161.

Yokota, Y., T. Ishikawa, S.-I. Watanabe, T. Tashiro, and A. Asada (2016), Seafloor geodetic constraints on interplate coupling of the Nankai Trough megathrust zone, *Nature*, *534*(7607), 374–377, doi:10.1038/nature17632.

Yoshioka, S., and Y. Matsuoka (2013), Interplate coupling along the Nankai Trough, southwest Japan, inferred from inversion analyses of GPS data: Effects of subducting plate geometry and spacing of hypothetical ocean-bottom GPS stations, *Tectonophysics*, *600*(C), 165–174, doi:10.1016/j.tecto.2013.01.023.

Yoshioka, S., Y. Matsuoka, and S. Ide (2015), Spatiotemporal slip distributions of three long-term slow slip events beneath the Bungo Channel, southwest Japan, inferred from inversion analyses of GPS data, *Geophysical Journal International*, *201*(3), 1437–1455, doi:10.1093/gji/ggv022.

Authors: 1) Francisco Ortega-Culaciati, Visiting Researcher, Research Center for Urban Safety and Security, Kobe University, Japan; 2) Francisco Ortega-Culaciati, Assistant Professor, Department of Geophysics, Faculty of Physical and Mathematical Sciences, University of Chile; 3) Shoichi Yoshioka, Professor, Research Center for Urban Safety and Security, Kobe University, Japan; 4) Takahiro Akiyama, Graduate School of Science, Faculty of Science, Kobe University, Japan.

© 2019 Research Center for Urban Safety and Security, Kobe University. All rights reserved.